Aquaporin 0−Calmodulin Interaction and the Effect of Aquaporin 0 Phosphorylation†

K. M. Lindsey Rose, Z. Wang, G. N. Magrath, E. S. Hazard, J. D. Hildebrandt, and K. L. Schey*

Department of Cell and Molecular Pharmacology, 173 Ashley Avenue, Medical University of South Carolina, Charleston, South Carolina 29425

Received October 2, 2007; Revised Manuscript Received October 30, 2007

ABSTRACT: Aquaporin 0 (AQP0), also known as major intrinsic protein of lens, is the most abundant membrane protein in the lens and it undergoes a host of C-terminally directed posttranslational modifications. The C-terminal region containing the major phosphorylation sites is a putative calmodulin-binding site, and calmodulin has been shown to regulate AQP0 water permeability. The purpose of the present study was to elucidate the role of AQP0 phosphorylation on calmodulin binding. AQP0 C-terminal peptides were synthesized with and without serine phosphorylation on S231 and S235, and the ability of these peptides to bind dansyl-labeled calmodulin and the calcium dependence of the interaction was assessed using a fluorescence binding assay. The AQP0 C-terminal phosphorylated peptides were found to have 20−50-fold lower affinities for calmodulin than the unphosphorylated peptide. Chemical cross-linking studies revealed specific sites of AQP0−calmodulin interaction that are significantly reduced by AQP0 phosphorylation. These data suggest that AQP0 C-terminal phosphorylation affects calmodulin binding in vivo and has a role in regulation of AQP0 function.

Aquaporin 0 (AQP0), also known as major intrinsic protein (MIP), is the most abundant membrane protein in the ocular lens and is expressed in lens fiber cells (*1*). AQP0 belongs to the aquaporin family of water channel proteins, which possess six transmembrane-spanning α-helical regions with their N- and C-termini located intracellularly (*2*). AQP0 functions as a water-permeable channel (*3*−*6*), has a role in fiber cell adhesion (*7*−*9*), and is essential for lens transparency (*10*). AQP0 mutations in humans and mice cause optical dysfunction and result in the formation of cataract (*11*−*17*). In addition, lenses of AQP0-knockout mice have cataract, as well as optical defects, decreased fiber cell water permeability, and abnormal fiber cell structure (*10*, *18*). These effects resulting from mutations and deficiency of AQP0 demonstrate AQP0's critical roles in development and maintenance of lens transparency and function.

In studies of aged lenses, a multitude of AQP0 posttranslational modifications have been identified primarily on the C-terminus. Abundant C-terminal truncation and deamidation have been reported as well as significant phosphorylation at serines 229, 231, and 235 (*19*, *20*). While the abundance of modifications make the AQP0 C-terminus an interesting region of the protein, the C-termini are also the most structurally diverse regions among the aquaporins and are thought to play tissue-specific regulatory roles.

Numerous studies have examined the involvement of aquaporin C-termini in regulation of protein function, and the most studied regulatory mechanism for aquaporins involving the C-terminus is the shuttling of AQP2 in the renal collecting duct. Vasopressin-stimulated PKA phosphorylation of the AQP2 C-terminal tail is required for shuttling to the apical membrane (*21*, *22*). However, there is no evidence for AQP0 shuttling in the lens. Calcium has also been implicated in the regulation of AQP1 function (*23*), and roles for calcium and calmodulin have been demonstrated in AQP2 (*24*) and AQP0 function (*25*−*27*). While high calcium increased the water permeability of endogenous AQP0 in fiber cell membrane vesicles (*26*), the opposite effect on permeability was shown with exogenously expressed AQP0 in oocytes (*25*−*27*). Furthermore, treatment with calmodulin inhibitors greatly reduced the calcium effects on AQP0 water permeability in both oocytes and fiber membrane vesicles (*25*, *26*).

Calmodulin is the most ubiquitous member of the family of calcium regulatory proteins, and over 80 calmodulin-regulated proteins have been identified (*28*). A possible calmodulin binding site has been identified within bovine AQP0 C-terminal residues 223−242 (*29*), a region containing known phosphorylation sites. Thus, if this sequence is, in fact, part of a calmodulin binding site, its phosphorylation may regulate this binding interaction. Here, a fluorescent binding assay was used to test whether this sequence has calmodulin-binding activity and whether or not this is altered by phosphorylation. Subsequent studies used chemical cross-linking and molecular modeling to identify the region of interaction of the peptide with calmodulin. The results provide detailed molecular information on CaM−AQP0 interactions and lead to a more thorough understanding of the regulation of water permeability of AQP0.

† Support came from the NIH (EY-13462; EY-14793, GM-67084) and the Kilpatrick Medical Research Fund.

* Corresponding author. Phone: (843)792-2471. Fax: (843)792-2475. E-mail: scheykl@musc.edu.

10.1021/bi701980t CCC: $40.75
Published on Web 12/15/2007

MATERIALS AND METHODS

Synthesis of AQP0 C-Terminal Peptides. Four peptides identical to the human AQP0 C-terminal sequence, residues 224−241 (FPRLKSISERLSVLKGAK) unmodified, S235 phosphorylated, 231 phosphorylated, and S235/S231 doubly phosphorylated, were synthesized at the MUSC Proteogenomics facility using standard solid-phase methods. An AQP0 extracellular loop peptide, corresponding to human AQP0 residues 110−127 with sequence CPAVRGNLALNTLHPAVSV, was also synthesized for use as a negative control. Bovine analogs were synthesized by EZBiolab (Westfield, IN). Peptides were purified by reconstitution in distilled H_2O (dH_2O), incubation on C18 Sep-Paks (Waters), washing with dH_2O, and elution with 75% acetonitrile. After peptides were vacuum-dried, they were reconstituted in 100 mM Tris, pH 7.5. The purity of the peptides was verified using MALDI time-of-flight (TOF) analysis on a Voyager DE-STR TOF mass spectrometer (Applied Biosystems). Peptide concentrations were determined using the BCA protein assay method (Pierce).

Dansyl Conjugation to Calmodulin. Purified bovine brain calmodulin (Calbiochem), 1 mg, lyophilized from a 150 mM NaCl, 2 mM EDTA solution, was reconstituted in 0.6 mL of dH_2O and filtered using a 10 000 MW cutoff filter (Millipore). To ensure complete buffer exchange and removal of EDTA, 0.6 mL of 100 mM sodium bicarbonate (pH 9.6) was used to dilute the centrifugal filter retentate and to filter the calmodulin solution. This filtering procedure was repeated three times. Calmodulin was labeled with the dansyl fluorophore by incubating calmodulin (1 mg) with dansyl chloride (5-dimethylaminonaphthalene-1-sulfonyl chloride; Molecular Probes) in a 1:6 molar ratio in 100 mM sodium bicarbonate (pH 9.6) for 1.5 h at 4 °C with constant agitation. Dansyl chloride, 300 μg, was first solubilized in 30 μL of acetone, and 10 μL was added to the final 0.6 mL of filtered calmodulin in sodium bicarbonate. Excess dansyl reagent was removed and dansyl-calmodulin (dansyl-CaM) was exchanged to 100 mM Tris (pH 7.5) by filtering the reaction mixture three times using another 10 000 MW cutoff centrifugal filter. Dansyl-CaM labeling was monitored by MALDI TOF mass spectrometry, and one or two dansyl groups were conjugated per calmodulin molecule. Dansyl-CaM concentration was determined by the BCA protein assay method, and a 0.6 mL of stock solution of approximately 90 μM was attained after each dansyl-CaM conjugation.

Fluorescence Spectroscopy with Dansyl-CaM. With the exception of the calcium dependence studies, fluorescence measurements were performed with a SLM 8000C spectrofluorometer (Aminco-Bowman). A microcuvette (Starna Cells, Inc.) of path length 4 mm and a volume of about 200 μL was used, and measurements were made at room temperature. A final concentration range from 0 to 30 μM of the AQP0 C-terminal peptides, the negative control AQP0 extracellular loop peptide, and a positive control myosin light chain kinase peptide (*30*) (Calbiochem; cat. no. 208735) were incubated with dansyl-CaM in 100 mM Tris (pH 7.5) with 0.15 mM $CaCl_2$ for 1 h at room temperature. The concentration of dansyl-CaM was varied from 0.1 to 0.5 μM. After excitation of the dansyl moiety at 340 nm, fluorescence emission spectra of dansyl-CaM were measured from 400 to 600 nm with a measurement taken every nanometer with an integration time of 1 s. To titrate the dansyl-CaM fluorescence with increasing peptide concentrations, fluorescence emission at 495 nm was acquired for each peptide concentration. Data points at 495 nm corresponded to the average of approximately 10 emission measurements integrated over 1 s, and the data points were acquired from duplicate samples.

Calcium Dependence of CaM and AQP0 Interaction. Peptides, dansyl-calmodulin, and $CaCl_2$ were dissolved in 100 mM Tris buffer containing 100 μM EGTA (pH 7.5). A final concentration of 8 μM of AQP0 C-terminal peptide or MLCK was mixed with 0.3 μM of dansyl-calmodulin and a series of $CaCl_2$ concentrations (0−150 μM). Free Ca^{2+} concentration was calculated using a Web-based tool (http://entropy.brneurosci.org/egta.html) assuming no Ca^{2+} and Mg^{2+} in the system without adding $CaCl_2$. Tris buffer containing 100 μM EGTA (pH 7.5) was used to bring the total volume to 200 μL. The solutions were incubated at room temperature for 1 h and fluorescence emission spectra were measured from 400 to 600 nm with excitation wavelength at 340 nm (OLIS DM45 spectrofluorometer). Three replicates were measured with each Ca^{2+} concentration. Peptide-bound and free calmodulin signals were resolved with this spectrofluorometer; therefore, the fluorescence intensity at wavelength (476 nm for MLCK and 482 nm for APQ0 peptide) was plotted against the calculated free Ca^{2+} concentration (in log 10 scale).

Affinity Constant Determination for AQP0 C-Terminal Peptide Binding to Calmodulin. Emission measurements at 495 nm were fit to concentration−response curves using the Boltzmann one-site binding equation to attain dissociation constants (K_D) for each of the peptides (*31*). Data points of dansyl-CaM emission in the absence of peptide were used for the baseline of the sigmoidal Boltzmann curve. The top of the sigmoidal curve was determined following titration of dansyl-CaM emission with high concentrations of peptide. Dissociation constants for the phosphorylated peptides were found to be equivalent to the EC_{50} values obtained from the fitted Boltzmann curves for each dansyl-CaM concentration. Because of the relatively higher affinity binding of the unphosphorylated peptide, EC_{50} values at various dansyl-CaM concentrations were fit by linear regression and extrapolated to zero dansyl-CaM concentration to attain the K_D (*y*-intercept) (*31*). Each K_D value (micromolar) determined was converted to its log value, and the mean and the standard errors of the means (SEM) of the log values were calculated for each AQP0 C-terminal peptide. To test for statistically significant differences, analysis of variance (ANOVA) and Tukey's HSD tests were used to make multiple comparisons among the four peptides.

Chemical Cross-Linking of APQ0 224−241 to Calmodulin. Bovine brain calmodulin was desalted using a 10 000 MW cutoff filter as described above. CaM and AQP0 peptides (residues 224−241 unphosphorylated, S235 phosphorylated, and 231/235 phosphorylated) were reconstituted in 50 mM potassium phosphate buffer (pH 7.4) and mixed in a 1:5:7.5 molar ratio of CaM/peptide/$CaCl_2$ to a final CaM concentration 20 μM. The mixture was incubated at room temperature for 1 h, after which 1-ethyl-3-[3-dimethylaminopropyl]-carbodiimide hydrochloride (EDC, Pierce) was added to the mixture at a concentration of 2 mM. The cross-linking reaction was conducted at room temperature for 2 h. The excess amounts of cross-linker and peptides were removed

by washing with water six times using 10 000 MW cutoff filter. The protein remaining on the filter was dissolved in water and dried via Speedvac.

Trypsin Digestion. A 17.5 μg portion of CaM after cross-linking reaction was dissolved in 100 μL of 50 mM ammonium bicarbonate buffer (pH 8) and 1 μg of trypsin was added. The digestion was performed at 37 °C for 24 h. The digestion was stopped by adding TFA to 0.1%, and the samples were dried and stored at −20 °C until further analysis.

Mass Spectrometry Analysis. MALDI-TOF mass spectrometry of the cross-linking reaction mixture was performed on a Voyager DE-STR TOF mass spectrometer (Applied Biosystems). Samples were prepared by mixing 0.5 μL of sample solution and 0.5 μL of sinapinic acid solutions and spotted on a MALDI sample plate. Thioredoxin (*Escherichia coli*, MW = 11674.5) and apomyoglobin (equine, MW = 16952.6) were used as standards for mass calibration. Trypsin-digested peptides were reconstituted in H_2O (0.1% TFA) and analyzed by HPLC−ESI-MS. Trypsin peptides were separated on an Ultimate NanoLC system. Samples were desalted over a trapping column (PepMap, C18, 5 μm, 300 μm i.d. × 5 mm, 100 Å) for 4 min with 20 μL/min flow rate and then loaded on the separation column (PepMap C18, 150 mm × 75 μm, 3 μm, 100 Å, Dionex) using the following gradient with 0.18 μL/min flow rate: 0−80 min, 2−50% ACN (0.02% HFBA); 80−100 min, 50−95% ACN (0.02% HFBA). Tandem mass spectra of cross-linked peptides were interpreted manually.

The relative percentage of cross-linking was calculated by calculating the ratio of peak areas of cross-linked peptide signals versus the non-cross-linked calmolulin peptide. Peak areas were obtained from selected ion chromatograms of each mass-to-charge ratio of a predicted peptide. The chromatogram was subjected to three-point boxcar smoothing using the Qual Browser Program of the Thermo Finnigan Xcalibur software. Peak area integration was accomplishing using Xcalibur's default options.

Molecular Model. A 1.7 Å resolution calmodulin structure (PDB ID 1MXE) from fruitfly calmodulin with calmodulin kinase bound was used, as calmodulin sequences are nearly completely conserved among all species (note that in human calmodulin E14, D78, D80 and E84 are perfectly preserved). The aquaporin 0 structure employed corresponds to human AQP0 227−241 (LKSISERLSVLKGAK). The native structure for this aquaporin sequence (only residues 227−238 are in the structure file) was extracted from the electron crystallographic structure (PDB ID 2B6O) with the SYBYL Biopolymer module (Tripos Inc., St. Louis, MO). The helix of the calmodulin kinase peptide bound in the original structure was deleted and the human AQP0 peptide structure placed into the vacancy. The AQP0 peptide structure was manually adjusted to place cross-linked lysine (K228) in the general vicinity of residues D78, D80, and E84. In order to remove steric clashes, hydrogen atoms and AMBER charges were added; Ca atoms were assigned a +2 charge. The system was minimized until the energy gradient reached 0.05 kcal mol^{-1} using the AMBER force field (AMBER_FF99) as implemented in the SYBYL Biopolymer module.

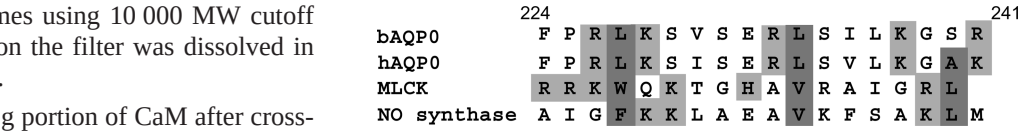

FIGURE 1: Sequence alignment of the known calmodulin-binding domains of smooth muscle MLCK and neuronal nitric oxide synthase with human and bovine AQP0 residues 224−241. Light gray shaded boxes indicate positively charged residues. Dark gray shaded boxes indicate key hydrophobic residues in the 1−8−14 calmodulin-binding motif.

RESULTS

Dansyl-Calmodulin as a Reporter for Peptide/Calmodulin Interactions. Dansyl-calmodulin is a well-characterized reporter for peptide interactions with calmodulin. While fluorescence emission of dansyl-CaM in the absence of an interacting peptide is maximal at 510 to 520 nm, the addition of an interacting peptide blue shifts the emission maximum to 495 to 500 nm and increases the fluorescence intensity of the dansyl moiety (*32*). These changes in dansyl-CaM fluorescence are caused by an increase in hydrophobic (protein) environment around the dansyl fluorophore and a subsequent increase in the quantum yield of dansyl fluorescence after substrate binding as previously shown for myosin light chain kinase (MLCK), the plasma membrane Ca^{2+} pump, adenylyl cyclase, nitric oxide synthase, the Na^+/H^+ exchanger NHE1, and the 5-HT_{1A} receptor (*31*−*36*).

Selection of Human AQP0 C-Terminal Peptide 224−*241.* The AQP0 C-terminal peptide used for the dansyl-CaM binding studies corresponds to human AQP0 residues 224−241. Aside from the fact that residues 224−241 in human AQP0 contain three serine phosphorylation sites of interest, these specific residues were selected on the basis of a previous study of calmodulin binding to a synthetic peptide mimicking bovine AQP0 223−242 (*29*) and on the results of a computer prediction program (University of Toronto) (*37*) that identifies putative calmodulin-binding domains based on such physical characteristics as α-helical propensity, residue charge, and hydrophobic residue content. In Figure 1, the human and bovine AQP0 peptide sequences are aligned with two other calmodulin-binding domains from MLCK and nitric oxide synthase. Positively charged residues (Figure 1, shaded light gray) and key hydrophobic residues (Figure 1, shaded dark gray) are indicated within the sequence. The calmodulin binding domains of MLCK and nitric oxide synthase have been classified into the calcium-dependent 1−8−14 binding motif subclass, and the AQP0 sequence has high homology with this motif.

Interaction of Dansyl-Calmodulin with the AQP0 C-Terminal Peptide. To evaluate the ability of AQP0 224−241 to bind dansyl-CaM, changes in the fluorescence emission of dansyl CaM with addition of the AQP0 C-terminal peptide were compared to the emission changes seen with addition of a known calmodulin-binding domain of MLCK and with addition of a negative control peptide. As shown in Figure 2, dansyl-CaM alone (Figure 2; solid line) in 100 mM Tris, 0.15 mM $CaCl_2$ has an emission maximum of 510 nm. After incubation with the positive control MLCK peptide (Figure 2; open diamonds), dansyl-CaM emission blue shifts to 495 nm and increases in fluorescence by a factor of 1.4, indicating a physical association with calmodulin. Similar to the MLCK peptide, the AQP0 C-terminal unphosphorylated peptide at

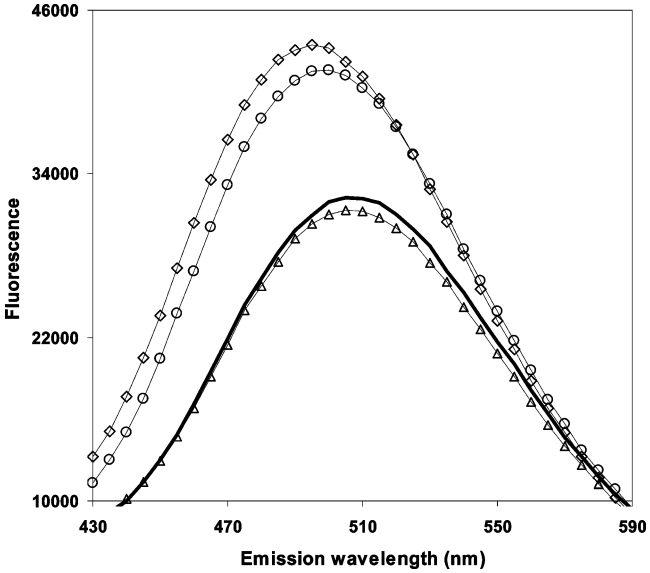

FIGURE 2: Fluorescence emission spectra of dansyl-calmodulin alone and after incubation with either the positive control MLCK peptide, the negative control AQP0 110−127 extracellular loop peptide, or the human AQP0 C-terminal peptide. The dansyl-CaM concentration was 0.3 μM, the peptide concentration was 8 μM, and the total calcium concentration was 0.15 mM. Dansyl emission was measured after excitation at 340 nm. Key: dansyl-CaM alone (solid line), dansyl-CaM + MLCK (◊), dansyl-CaM + AQP0 C-terminal peptide (○), dansyl-CaM + AQP0 loop peptide (△). Binding of peptides to dansyl-CaM causes a blue-shift and increase in fluorescence from 510 to 495 nm. Each data point is an average of 10 measurements and each spectrum was acquired in duplicate.

the same concentration (Figure 2, open circles) also resulted in a blue shift and a 1.3-fold increase in fluorescence. In contrast, dansyl emission neither blue-shifted nor increased in fluorescence after addition of the negative control AQP0 extracellular loop peptide (Figure 2, open triangles), indicating a lack of interaction between this peptide and dansyl-CaM. Note that nearly identical results were obtained for the bovine AQP0 peptide (data not shown), indicating that the conserved substitutions between human and bovine sequences do not alter the CaM−AQP0 interaction.

Calcium Dependence of AQP0 C-Terminal Peptide/Calmodulin Interaction. While the calmodulin-binding site on AQP0 is known to reside in the C-terminus, the Ca^{2+} dependence of this AQP0/CaM interaction is controversial. Although several studies using ^{125}I−CaM binding assays and cross-linking methods have shown that CaM binds to AQP0 in the presence of Ca^{2+} (*38*−*40*), other studies using circular dichroism and tryptophan fluorescence suggested that Ca^{2+}-free CaM (apo-CaM) binds AQP0 (*29*). In particular, the bovine AQP0 peptide study reported a significant change in the CD spectra due to α-helical content when apo-CaM and the bovine AQP0 peptide were combined, suggesting their interaction (*29*). Moreover, the addition of Ca^{2+} substantially changed the CD spectrum further, indicating additional conformational changes (*29*).

Therefore, the dansyl-CaM fluorescence assay was used to examine the calcium sensitivity of the unphosphorylated AQP0 C-terminal peptide−CaM interaction. Again, the MLCK peptide was used as a positive control. The results using 0.3 μM CaM and 8 μM peptide concentrations are shown in Figure 3 and clearly indicate a calcium dependence on the dansyl-CaM fluorescence. Fitting the curve to the Hill

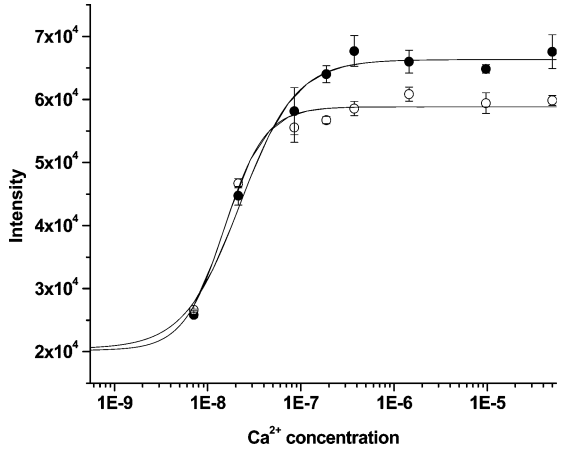

FIGURE 3: Calcium-dependent interaction of dansyl-calmodulin with the MLCK and AQP0 peptides. The dansyl-CaM (0.3 μM) fluorescence at 482 nm following incubation with the unphosphorylated AQP0 C-terminal peptide (○) and the dansyl-CaM fluorescence at 476 nm following incubation with the MLCK (●) peptide was measured as a function of the calcium concentration (peptide concentrations were 8 μM). Data were acquired on the Olis DM45 spectrofluorometer and are plotted as a function of calculated free calcium concentration. Each curve was measured in triplicate.

equation gave Hill coefficients of 2.2 and 2.0 for calcium binding in the presence of the AQP0 and MLCK peptides, respectively, indicating expected positive cooperativity. These values are similar to the Hill coefficient of 2.1 reported in the presence of a caldesmon fragment (*41*). The $pCa_{0.5}$ values calculated from the data are 7.82 and 7.69 in the presence of the AQP0 and MLCK peptides, respectively. The phosphorylated S235P peptide had significantly lower binding (see discussion below) even at saturating calcium concentrations; therefore, a full calcium titration curve was not acquired.

Effect of Phosphorylation of AQP0 224−*241 on Calmodulin Binding.* Phosphorylation sites on the C-terminus of human AQP0 have previously been identified by mass spectrometric analysis and include serines 229, 231, and 235 (*20*). S235 was identified as the most abundant phosphorylation site, while S231 and S229 were phosphorylated to a lesser degree. Since these phosphorylation sites are in the predicted calmodulin-binding site, it is important to determine the effect of phosphorylation on calmodulin binding. While typical calmodulin-binding domains have few or no negatively charged residues, single and double phosphorylation of AQP0 224−241 would add a single and double negative charge, respectively, to this calmodulin-binding region. The binding of dansyl-CaM to the serine 235-phosphorylated AQP0 peptide (S235-P) indicated a reduction in binding, as illustrated in Figure 4 (filled triangles), when compared to the results seen with the unphosphorylated AQP0 peptide (open circles). The dansyl-CaM emission after incubation with the S235-P peptide at the same concentration is less blue-shifted and lower in fluorescence intensity than emission after incubation with the unphosphorylated peptide. Dansyl-CaM incubation with the serine-231-phosphorylated peptide (S231-P) resulted in a similar emission spectrum (Figure 4, open squares) to that of S235-P, indicating a similar reduction in calmodulin binding. Moreover, double phosphorylation of both serines 235 and 231 (Figure 4, filled circles) further reduced the ability of the AQP0 C-terminal peptide to bind

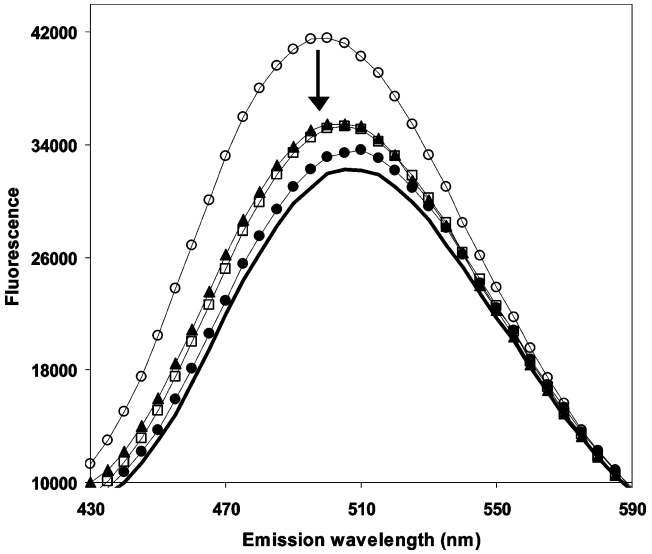

FIGURE 4: Fluorescence emission spectra of dansyl-calmodulin alone and with either the unphosphorylated AQP0 peptide or the serine-phosphorylated peptide analogues. The dansyl-CaM concentration was 0.3 μM, the peptide concentration was 8 μM, and the total calcium concentration was 0.15 mM. Key: dansyl-CaM emission alone (solid line), dansyl-CaM + AQP0 unphosphorylated peptide (○), dansyl-CaM + AQP0 S235 phosphorylated (▲), dansyl-CaM + AQP0 S231 phosphorylated (□), and dansyl-CaM + AQP0 doubly phosphorylated (●). The arrow indicates the decrease in association of the phosphorylated peptides with dansyl-CaM as compared to the unphosphorylated AQP0 peptide. Each data point is an average of 10 measurements and each spectrum was acquired in duplicate.

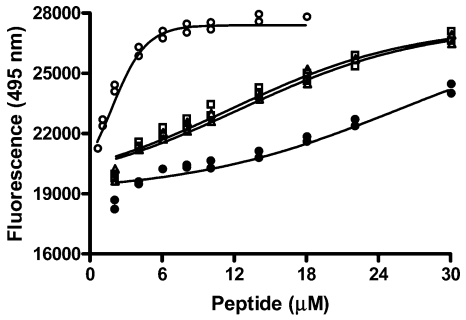

FIGURE 5: Fluorescence titrations of dansyl-calmodulin with unphosphorylated and phosphorylated AQP0 224−241. Concentration-dependent enhancement of 0.3 μM dansyl-CaM fluorescence was measured at an emission wavelength of 495 nm, and a total calcium concentration of 0.15 mM. Dansyl-CaM was incubated with increasing concentrations of the AQP0 peptides (0−30 μM), and measurements were fit to the Boltzmann equation. Key: dansyl-CaM + AQP0 unphosphorylated (○), dansyl-CaM + AQP0 S235 phosphorylated (△), dansyl-CaM + AQP0 S231 phosphorylated (□), dansyl-CaM + AQP0 doubly phosphorylated (●). Each curve was acquired in duplicate (all data points plotted) and the entire experiment was done in quadruplicate.

dansyl-CaM. These results suggest that C-terminal phosphorylation of AQP0 reduces the affinity of AQP0 for calmodulin.

To compare the concentration-dependent binding of the AQP0 peptides to dansyl-CaM, the dansyl-CaM emission was titrated with increasing concentrations of the peptides, and the emission measurements at 495 nm were fit to the Boltzmann one-site binding equation. As illustrated in Figure 5, the unphosphorylated peptide (open circles) at a concentration of 6 μM caused near saturation of the emission of dansyl-CaM (0.3 μM). In contrast, the dansyl-CaM emissions

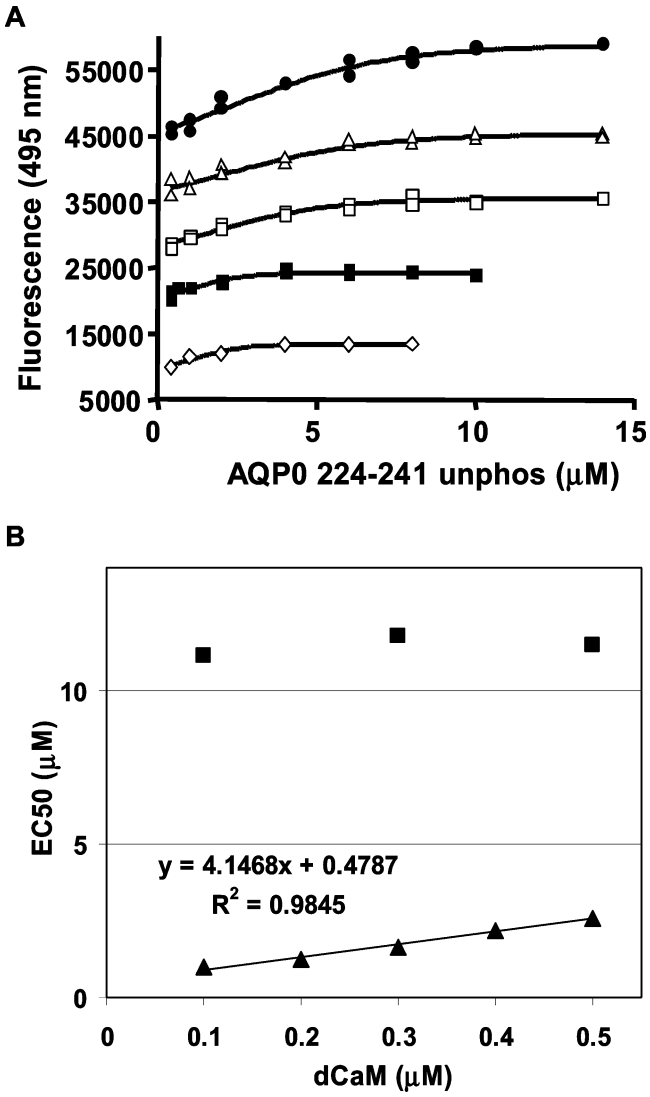

FIGURE 6: (A) Fluorescence titrations of a range of dansyl-calmodulin concentrations with the unphosphorylated AQP0 C-terminal peptide. Emission measurements of dansyl-CaM at concentrations of 0.1 (◊), 0.2 (■), 0.3 (□), 0.4 (△), and 0.5 (●) μM, respectively, and a total calcium concentration of 0.15 mM. (B) K_D determination of the AQP0 peptides for dansyl-calmodulin. EC_{50} values of the unphosphorylated peptide (▲) and the S235-P peptide (■) with each concentration of dansyl-CaM for one of four sets of experiments are shown. Linear regression was used to extrapolate the K_D of the calmodulin−unphosphorylated AQP0 peptide interaction and gives a K_D of 0.48 μM.

after incubation with an equivalent concentration of the singly S235 (Figure 5; open triangles) and S231 (Figure 5; open squares) phosphorylated peptides have not approached even half-maximal saturation. Furthermore, final concentrations of 30 μM S235-P and S231-P were required in order to approach complete saturation of dansyl emission. In greater contrast, the doubly phosphorylated peptide (Figure 5; filled circles) has only reached half-maximal titration of dansyl emission at a 30 μM concentration.

Affinity Constants of the AQP0 C-Terminal Peptides for Dansyl-Calmodulin. Upon performing dansyl-CaM titrations at a range of dansyl-CaM concentrations with the AQP0 unphosphorylated peptide, the EC_{50} of the unphosphorylated peptide was found to be dependent on the concentration of dansyl-CaM. Titration of 0.1−0.5 μM dansyl-CaM with the unphosphorylated peptide is demonstrated in Figure 6A. With

Table 1: Summary of Chemical Cross-Linking Results

CaM peptides	AQP0 peptides	wild type Ratio[a]	S235P Ratio	S231P S235P Ratio
78−86 (E84, D80)[b,c]	234−241 (K238)	1.3	N/D	N/D
78−86 (D78, E84)[b]	227−233 (K228)	3.2	0.38	N/D
76−86 (D78, E84)[b]	227−233 (K228)	0.80	N/D	N/D
14−30 (E14)	234−241 (K238)	0.33	N/D	N/D

[a] The ratios report peak area of cross-linked CaM peptides/peak area of non-cross-linked CaM peptides. [b] Non-cross-linked CaM peptides abundances included CaM 78−86 and miscleaved peptides 76−86 and 78−90. [c] Cross-linked residues indicated in parentheses.

successively higher concentrations of dansyl-CaM, a higher concentration of unphosphorylated peptide is required to saturate dansyl-CaM emission. This phenomenon of ligand affinity constants being dependent on dansyl-CaM concentrations has been documented previously and was shown to be characteristic of high-affinity binding of calmodulin (*31*, *42*). Therefore, using the Boltzmann equation, we first determined the concentration of the unphosphorylated peptide required for half-maximal saturation of dansyl-CaM emission for each dansyl-CaM concentration. These EC_{50} values were then fit by linear regression, and the K_D was obtained after extrapolation to an infinitely low concentration of dansy-CaM. Linear regression analysis and the K_D determination of the unphosphorylated peptides are shown in Figure 6B (filled triangles). Affinity constants were calculated and averaged after linear regression of four data sets using the concentration range of 0.1−0.5 μM dansyl-CaM. A K_D of 0.5 μM for dansyl-CaM was determined for the unphosphorylated AQP0 peptide.

A similar analysis for the EC_{50} values of the S235-P peptide at various dansyl-CaM concentrations is also shown in Figure 6B (filled squares). In contrast to the unphosphorylated AQP0 peptide results, the S235-P EC50 values do not linearly increase with increasing dansyl-CaM, indicating that S235-P has low-affinity binding of dansyl-CaM. As a result, K_D values for the phosphorylated peptides were taken to be equivalent to the calculated EC_{50} values and did not require linear regression analysis. Single phosphorylation of AQP0 224−241 at either S235 or S231 significantly increased the K_D of AQP0 224−241 for dansyl-CaM from 0.5 to 12.2 and 10.5 μM, respectively. Thus, the singly phosphorylated peptides have an approximate 20-fold reduction in binding affinity. Again, similar results were obtained with the bovine AQP0 peptides (not shown). Double phosphorylation increased the K_D of the AQP0 peptide to 24.5 μM and thus causes a 50-fold reduction in binding affinity for dansyl-CaM. With 95% confidence, the K_D values (μM) of the unphosphorylated, S235 phosphorylated, S231 phosphorylated, and doubly phosphorylated AQP0 peptides reside within the intervals of (0.426,0.591), (12.084,12.362), (9.883,11.230), and (23.385,25.723), respectively.

Chemical Cross-Linking of CaM and AQP0 Peptides. In order to identify sites of CaM/AQP0 interactions, chemical cross-linking studies with the zero-length bifunctional cross-linker EDC were undertaken with CaM and AQP0 224−241. Spectral interpretation of tandem mass spectra from LC/MS/MS analysis of tryptic digests of cross-linked protein indicated the location of cross-linked residues between CaM and AQP0 (spectra available in Supporting Information). The results, summarized in Table 1, showed cross-linking of basic residues from the AQP0 peptide (K228 and K238) with acidic residues on CaM (D78, D80, E84, and E14). Note that several calmodulin peptides were observed as cross-linked to the APQ0 peptide due to miscleavage by trypsin. Further note that multiple cross-linked sites were observed for a given peptide; for example, the AQP0 peptide cross-linked most efficiently to calmodulin peptide 78−86, but both residues D78 and E84 of calmodulin were observed as cross-linked to AQP0 residue K228. The observation that AQP0 K238 cross-linked to both E14 and E80/E84 of calmodulin suggests that the AQP0 could bind in a forward and a reverse direction (see modeling studies below). Note that cross-linking with the bovine AQP0 peptide gave nearly identical results (not shown). Furthermore, the singly phosphorylated AQP0 peptide showed decreased cross-linking efficiency at the observed sites and the doubly phosphorylated AQP0 peptide showed no cross-linking to CaM. These results are consistent with the fluorescent binding studies and the calculated affinity constants for unmodified and phosphorylated AQP0 peptides described above.

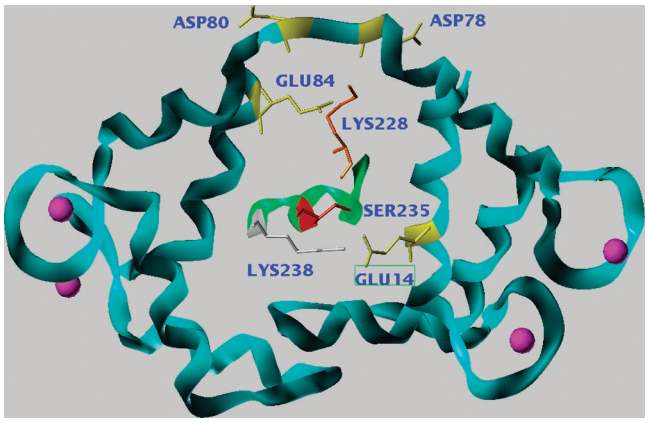

FIGURE 7: Molecular model of AQP0 peptide bound calmodulin. Molecular structure of AQP0 peptide bound to calmodulin indicating calmodulin residues (yellow) and residues of the AQP0 peptide (orange and white) that were observed to be chemically cross-linked in mass spectrometry studies. Pink spheres indicate calcium ions.

A molecular model was generated, using chemical cross-linking results as a guide for AQP0 peptide placement, to aid in visualization of cross-linked residues in the calmodulin binding pocket. By replacing a CaM kinase peptide in the original PDB database structure with the AQP0 224−241 peptide, the resulting model (Figure 7) indicates the close proximity of the observed cross-linked residues. Calmodulin residues D78, D80, and E84 are in close proximity to and are cross-linked most efficiently to AQP0 K228 (Table 1). Although there is some cross-linking between these calmodulin residues and AQP0 K238, the efficiency is lower and may indicate a finite probability of the small peptide inserting into the binding pocket in a forward and reverse direction. Moreover, the cross-linking of calmodulin E14 was only observed to AQP0 K238, consistent with the K228 results.

DISCUSSION

The goal of this study was to compare the binding affinities of the unphosphorylated and phosphorylated human AQP0 C-terminal peptides for calmodulin (CaM) and to identify sites of interaction. The calculated K_D of the unphosphorylated peptide is approximately 500 nM, which differs from the reported K_D of 10 nM in a previous study using a bovine AQP0 peptide (*29*). However, the K_D reported for the bovine AQP0 peptide was determined using a modified bovine sequence with leucine 223 replaced by a tryptophan (Trp) residue for the tryptophan fluorescence emission assay. This substitution likely resulted in higher affinity binding of CaM, as the presence of a Trp residue in the N-terminal portions of the CaM-binding domains of both MLCK and the plasma membrane Ca^{2+} pump has been shown to increase affinity for CaM up to 300-fold (*30*, *33*). While a K_D of 0.5 μM might be considered an intermediate affinity for CaM, this degree of affinity is typical of CaM-binding domains containing a leucine residue in position 1, as is the case for AQP0. For example, a CaM-binding region of the 5-HT_{1A} receptor contains a leucine in this position and also has a similar K_D of 1.7 μM (*31*).

A significant finding from the present study is that single phosphorylation of either serine-235 or serine-231 and double phosphorylation of both serines significantly reduced the binding affinity of AQP0 224−241 for dansyl-calmodulin. As predicted, the additional negative charge to the AQP0 C-terminus with one or more serine phosphorylations substantially alters CaM-binding properties. Of interest, CaM-binding domains of target proteins are often present within or near phosphorylation sites for serine/threonine protein kinases A and C (*43*). For example, phosphorylation of the 5-HT_{1A} receptor (*31*) and the plasma membrane Ca^{2+} pump (*44*) by PKC has been shown to reduce CaM binding and is proposed to cause dramatic changes in the function of these two proteins. While the kinases responsible for human AQP0 phosphorylation are unknown, S231 is within a PKC consensus sequence, and S235 is within a PKA consensus sequence. In addition, numerous studies have indicated PKA and PKC phosphorylation of bovine AQP0 (*45*−*48*).

Chemical cross-linking studies revealed specific sites of interaction between CaM acidic residues and AQP0 basic residues similar to other CaM binding partners. Although a small AQP0 peptide was employed in these studies for experimental convenience, the present results confirm present and previous fluorescent binding results and identify specific interacting residues.

The functional significance of our findings is highlighted by the emerging picture of the regulation of AQP0 permeability (*25*−*27*) and the unknown function of AQP0 phosphorylation identified in multiple studies of AQP0 modifications (*20*). Although the details of the mechanisms by which AQP0 function is regulated in the lens are unknown, the reports of calmodulin binding and calcium/calmodulin regulation of AQP0 permeability in oocytes and in lens fiber vesicles provide clues to one regulatory mechanism of AQP0 function. In work by Nemeth-Cahalan and Hall, elevated calcium decreased the water permeability of exogenously expressed AQP0 in *Xenopus* oocytes (*25*). In studies by Varadaraj et al., increased calcium decreased AQP0 permeability in oocytes but increased endogenous AQP0 water permeability in lens fiber cell vesicles (*26*). Importantly, both groups of investigators demonstrated that calmodulin inhibitors eliminate the calcium effect on AQP0 water transport, indicating that, in both ooctyes and vesicles, calcium effects are mediated by CaM (*25*, *26*). Therefore, with the knowledge of specific AQP0 phosphorylation sites, their effects on CaM binding, and the calcium dependence of interaction, pieces of the Ca^{2+}/CaM regulatory mechanism of AQP0 water permeability can begin to be assembled.

As proposed by Varadaraj and co-workers (*26*), calmodulin binding to AQP0 likely induces a conformational change in AQP0, which subsequently alters the open probability of the aquaporin pore. Results from the present study are consistent with Ca^{2+}-bound CaM having a higher affinity for the AQP0 C-terminus, and thus binding of Ca^{2+}/CaM likely increases AQP0 permeability. Furthermore, in light of the present results, we extend this proposal to include the regulation of Ca^{2+}/CaM control of AQP0 permeability by phosphorylation of the AQP0 CaM-binding site, i.e., phosphorylated AQP0 has reduced CaM-binding affinity and lower permeability.

In previous studies using mass spectrometry to estimate the extent of phosphorylated human AQP0, Ball et al. regional differences were observed with the highest reported levels of phosphorylation in the inner cortex (*20*). Considering these results, calmodulin regulation of AQP0 permeability may be differentially altered in different regions of the human lens through posttranslational modification. After denucleation of fiber cells, regulation of protein function via synthesis/degradation pathways is eliminated. Thus, regulation of lens protein function via posttranslational modification is emerging as an important regulatory mechanism, e.g., connexin cleavage reducing pH sensitivity of gap junction permeability (*49*). The regional differences in regulation via AQP0 phosphorylation likely play a significant role in the internal lens circulation system (*50*, *51*) and may be important for fiber cell maturation and the formation of a water transport barrier (*52*) at the cortex/nucleus interface. Clearly, as more precise spatially resolved measurements of AQP0 structure and function are made, more accurate details of the role of AQP0 in lens fiber cell volume regulation, a requirement for the maintenance of lens transparency and homeostasis, will be obtained.

ACKNOWLEDGMENT

The authors thank Dr. Rosalie Crouch for helpful and insightful discussions, Drs. Craig Beeson and Yiannis Koutalos for use of their spectrofluorometer instruments, Dr. Steve Rosenzweig for use of his GraphPad Software for binding analysis, the MUSC Mass Spectrometry facility, and the MUSC Proteogenomics facility for peptide synthesis.

SUPPORTING INFORMATION AVAILABLE

Tandem mass spectra of cross-linked CaM−AQP0 peptides. This material is available free of charge via the Internet at http://pubs.acs.org.

REFERENCES

1. Waggoner, P. R., and Maisel, H. (1978) Immunofluorescent study of a chick lens fiber cell membrane polypeptide, *Exp. Eye Res. 27*, 151−157.

2. Gonen, T., Sliz, P., Kistler, J., Cheng, Y., and Walz, T. (2004) Aquaporin-0 membrane junctions reveal the structure of a closed water pore, *Nature 429*, 193−197.
3. Mulders, S. M., Preston, G. M., Deen, P. M., Guggino, W. B., van Os, C. H., and Agre, P. (1995) Water channel properties of major intrinsic protein of lens, *J. Biol. Chem. 270*, 9010−9016.
4. Kushmerick, C., Rice, S. J., Baldo, G. J., Haspel, H. C., and Mathias, R. T. (1995) Ion, water and neutral solute transport in *Xenopus* oocytes expressing frog lens MIP, *Exp. Eye Res. 61*, 351−362.
5. Chandy, G., Zampighi, G. A., Kreman, M., and Hall, J. E. (1997) Comparison of the water transporting properties of MIP and AQP1, *J. Membr. Biol. 159*, 29−39.
6. Varadaraj, K., Kushmerick, C., Baldo, G. J., Bassnett, S., Shiels, A., and Mathias, R. T. (1999) The role of MIP in lens fiber cell membrane transport, *J. Membr. Biol. 170*, 191−203.
7. Dunia, I., Manenti, S., Rousselet, A., and Benedetti, E. L. (1987) Electron microscopic observations of reconstituted proteoliposomes with the purified major intrinsic membrane protein of eye lens fibers, *J. Cell Biol. 105*, 1679−1689.
8. Michea, L. F., de la Fuente, M., and Lagos, N. (1994) Lens major intrinsic protein (MIP) promotes adhesion when reconstituted into large unilamellar liposomes, *Biochemistry 33*, 7663−7669.
9. Fotiadis, D., Hasler, L., Muller, D. J., Stahlberg, H., Kistler, J., and Engel, A. (2000) Surface tongue-and-groove contours on lens MIP facilitate cell-to-cell adherence, *J. Mol. Biol. 300*, 779−789.
10. Shiels, A., Bassnett, S., Varadaraj, K., Mathias, R., Al-Ghoul, K., Kuszak, J., Donoviel, D., Lilleberg, S., Friedrich, G., and Zambrowicz, B. (2001) Optical dysfunction of the crystalline lens in aquaporin-0-deficient mice, *Physiol. Genom. 7*, 179−186.
11. Muggleton-Harris, A. L., Festing, M. F., and Hall, M. (1987) A gene location for the inheritance of the cataract Fraser (CatFr) mouse congenital cataract, *Genet. Res. 49*, 235−238.
12. Shiels, A., Griffin, C. S., and Muggleton-Harris, A. L. (1991) Immunochemical comparison of the major intrinsic protein of eye-lens fibre cell membranes in mice with hereditary cataracts, *Biochim. Biophys. Acta 1097*, 318−324.
13. Shiels, A., and Bassnett, S. (1996) Mutations in the founder of the MIP gene family underlie cataract development in the mouse, *Nat. Genet. 12*, 212−215.
14. Shiels, A., Mackay, D., Bassnett, S., Al-Ghoul, K., and Kuszak, J. (2000) Disruption of lens fiber cell architecture in mice expressing a chimeric AQP0-LTR protein, *FASEB J. 14*, 2207−2212.
15. Sidjanin, D. J., Parker-Wilson, D. M., Neuhauser-Klaus, A., Pretsch, W., Favor, J., Deen, P. M., Ohtaka-Maruyama, C., Lu, Y., Bragin, A., Skach, W. R., Chepelinsky, A. B., Grimes, P. A., and Stambolian, D. E. (2001) A 76-bp deletion in the Mip gene causes autosomal dominant cataract in Hfi mice, *Genomics 74*, 313−319.
16. Francis, P., Chung, J. J., Yasui, M., Berry, V., Moore, A., Wyatt, M. K., Wistow, G., Bhattacharya, S. S., and Agre, P. (2000) Functional impairment of lens aquaporin in two families with dominantly inherited cataracts, *Hum. Mol. Genet. 9*, 2329−2334.
17. Bateman, J. B., Johannes, M., Flodman, P., Geyer, D. D., Clancy, K. P., Heinzmann, C., Kojis, T., Berry, R., Sparkes, R. S., and Spence, M. A. (2000) A new locus for autosomal dominant cataract on chromosome 12q13, *Invest. Ophthalmol. Vis. Sci. 41*, 2665−2670.
18. Al-Ghoul, K. J., Kirk, T., Kuszak, A. J., Zoltoski, R. K., Shiels, A., and Kuszak, J. R. (2003) Lens structure in MIP-deficient mice, *Anat. Rec. 273A*, 714−730.
19. Schey, K. L., Little, M., Fowler, J. G., and Crouch, R. K. (2000) Characterization of human lens major intrinsic protein structure, *Invest. Ophthalmol. Vis. Sci. 41*, 175−182.
20. Ball, L. E., Garland, D. L., Crouch, R. K., and Schey, K. L. (2004) Post-translational modifications of aquaporin 0 (AQP0) in the normal human lens: Spatial and temporal occurrence, *Biochemistry 43*, 9856−9865.
21. van Balkom, B. W., Savelkoul, P. J., Markovich, D., Hofman, E., Nielsen, S., van der Sluijs, P., and Deen, P. M. (2002) The role of putative phosphorylation sites in the targeting and shuttling of the aquaporin-2 water channel, *J. Biol. Chem. 277*, 41473−9.
22. Deen, P. M., Van Balkom, B. W., Savelkoul, P. J., Kamsteeg, E. J., Van Raak, M., Jennings, M. L., Muth, T. R., Rajendran, V., and Caplan, M. J. (2002) Aquaporin-2: COOH terminus is necessary but not sufficient for routing to the apical membrane, *Am. J. Physiol. Renal Physiol. 282*, F330−40.
23. Fotiadis, D., Suda, K., Tittmann, P., Jeno, P., Philippsen, A., Muller, D. J., Gross, H., and Engel, A. (2002) Identification and structure of a putative Ca^{2+}-binding domain at the C terminus of AQP1, *J. Mol. Biol. 318*, 1381−1394.
24. Chou, C. L., Yip, K. P., Michea, L., Kador, K., Ferraris, J. D., Wade, J. B., and Knepper, M. A. (2000) Regulation of aquaporin-2 trafficking by vasopressin in the renal collecting duct. Roles of ryanodine-sensitive Ca^{2+} stores and calmodulin, *J. Biol. Chem. 275*, 36839−36846.
25. Nemeth-Cahalan, K. L., and Hall, J. E. (2000) pH and calcium regulate the water permeability of aquaporin 0, *J. Biol. Chem. 275*, 6777−6782.
26. Varadaraj, K., Kumari, S., Shiels, A., and Mathias, R. T. (2005) Regulation of aquaporin water permeability in the lens, *Invest. Ophthalmol. Vis. Sci. 46*, 1393−1402.
27. Nemeth-Cahalan, K. L., Kalman, K., and Hall, J. E. (2004) Molecular basis of pH and Ca^{2+} regulation of aquaporin water permeability, *J. Gen. Physiol. 123*, 573−580.
28. Gomes, A. V., Barnes, J. A., and Vogel, H. J. (2000) Spectroscopic characterization of the interaction between calmodulin-dependent protein kinase I and calmodulin, *Arch. Biochem. Biophys. 379*, 28−36.
29. Girsch, S. J., and Peracchia, C. (1991) Calmodulin interacts with a C-terminus peptide from the lens membrane protein MIP26, *Curr. Eye Res. 10*, 839−849.
30. Torok, K., and Trentham, D. R. (1994) Mechanism of 2-chloro-(ϵ-amino-Lys75)-[6-[4-(*N*,*N*-diethylamino)phenyl]-1,3,5-triazin-4-yl]calmodulin interactions with smooth muscle myosin light chain kinase and derived peptides, *Biochemistry 33*, 12807−12820.
31. Turner, J. H., Gelasco, A. K., and Raymond, J. R. (2004) Calmodulin interacts with the third intracellular loop of the serotonin 5-hydroxytryptamine1A receptor at two distinct sites: Putative role in receptor phosphorylation by protein kinase C, *J. Biol. Chem. 279*, 17027−17037.
32. Malencik, D. A., and Anderson, S. R. (1982) Binding of simple peptides, hormones, and neurotransmitters by calmodulin, *Biochemistry 21*, 3480−3486.
33. Vorherr, T., James, P., Krebs, J., Enyedi, A., McCormick, D. J., Penniston, J. T., and Carafoli, E. (1990) Interaction of calmodulin with the calmodulin binding domain of the plasma membrane Ca2+ pump, *Biochemistry 29*, 355−365.
34. Vorherr, T., Knopfel, L., Hofmann, F., Mollner, S., Pfeuffer, T., and Carafoli, E. (1993) The calmodulin binding domain of nitric oxide synthase and adenylyl cyclase, *Biochemistry 32*, 6081−6088.
35. Bertrand, B., Wakabayashi, S., Ikeda, T., Pouyssegur, J., and Shigekawa, M. (1994) The Na+/H+ exchanger isoform 1 (NHE1) is a novel member of the calmodulin-binding proteins. Identification and characterization of calmodulin-binding sites, *J. Biol. Chem. 269*, 13703−13709.
36. Anagli, J., Hofmann, F., Quadroni, M., Vorherr, T., and Carafoli, E. (1995) The calmodulin-binding domain of the inducible (macrophage) nitric oxide synthase, *Eur. J. Biochem. 233*, 701−708.
37. Yap, K. L., Kim, J., Truong, K., Sherman, M., Yuan, T., and Ikura, M. (2000) Calmodulin target database, *J. Struct. Funct. Genom. 1*, 8−14.
38. Louis, C. F., Hogan, P., Visco, L., and Strasburg, G. (1990) Identity of the calmodulin-binding proteins in bovine lens plasma membranes, *Exp. Eye Res. 50*, 495−503.
39. Swamy-Mruthinti, S. (2001) Glycation decreases calmodulin binding to lens transmembrane protein, MIP, *Biochim. Biophys. Acta 1536*, 64−72.
40. Jarvis, L. J., and Louis, C. F. (1995) Purification and oligomeric state of the major lens fiber cell membrane proteins, *Curr. Eye Res. 14*, 799−808.
41. Yazawa, M., Ikura, M., Hikichi, K., Ying, L., and Yagi, K. (1987) Communication between two globular domains of calmodulin in the presence of mastoparan or caldesmon fragment. Ca2+ binding and 1H NMR, *J. Biol. Chem. 262*, 10951−10954.
42. Johnson, J. D., and Wittenauer, L. A. (1983) A fluorescent calmodulin that reports the binding of hydrophobic inhibitory ligands, *Biochem. J. 211*, 473−479.
43. Rhoads, A. R., and Friedberg, F. (1997) Sequence motifs for calmodulin recognition, *FASEB J. 11*, 331−340.

44. Enyedi, A., Elwess, N. L., Filoteo, A. G., Verma, A. K., Paszty, K., and Penniston, J. T. (1997) Protein kinase C phosphorylates the "a" forms of plasma membrane Ca^{2+} pump isoforms 2 and 3 and prevents binding of calmodulin, *J. Biol. Chem. 272*, 27525−27528.
45. Johnson, K. R., Panter, S. S., and Johnson, R. G. (1985) Phosphorylation of lens membranes with a cyclic AMP-dependent protein kinase purified from the bovine lens, *Biochim. Biophys. Acta 844*, 367−376.
46. Louis, C. F., Johnson, R., Johnson, K., and Turnquist, J. (1985) Characterization of the bovine lens plasma membrane substrates for cAMP-dependent protein kinase, *Eur. J. Biochem. 150*, 279−286.
47. Johnson, K. R., Lampe, P. D., Hur, K. C., Louis, C. F., and Johnson, R. G. (1986) A lens intercellular junction protein, MP26, is a phosphoprotein, *J. Cell Biol. 102*, 1334−1343.
48. Garland, D., and Russell, P. (1985) Phosphorylation of lens fiber cell membrane proteins, *Proc. Natl. Acad. Sci. U.S.A. 82*, 653−657.
49. Lin, J. S., Eckert, R., Kistler, J., and Donaldson, P. (1998) Spatial differences in gap junction gating in the lens are a consequence of connexin cleavage, *Eur. J. Cell Biol. 76*, 246−250.
50. Mathias, R. T., Rae, J. L., and Baldo, G. J. (1997) Physiological properties of the normal lens, *Physiol. Rev. 77*, 21−50.
51. Donaldson, P., Kistler, J., and Mathias, R. T. (2001) Molecular solutions to mammalian lens transparency, *News Physiol. Sci. 16*, 118−123.
52. Moffat, B. A., Landman, K. A., Truscott, R. J., Sweeney, M. H., and Pope, J. M. (1999) Age-related changes in the kinetics of water transport in normal human lenses, *Exp. Eye Res. 69*, 663−669.

BI701980T